

Evolutionary dynamics on any population structure

Benjamin Allen^{1,2,3}, Gabor Lippner^{3,4}, Yu-Ting Chen^{2,3,5}, Babak Fotouhi^{2,6}, Naghme Momeni^{2,7}, Shing-Tung Yau^{3,8} & Martin A. Nowak^{2,8,9}

Evolution occurs in populations of reproducing individuals. The structure of a population can affect which traits evolve^{1,2}. Understanding evolutionary game dynamics in structured populations remains difficult. Mathematical results are known for special structures in which all individuals have the same number of neighbours^{3–8}. The general case, in which the number of neighbours can vary, has remained open. For arbitrary selection intensity, the problem is in a computational complexity class that suggests there is no efficient algorithm⁹. Whether a simple solution for weak selection exists has remained unanswered. Here we provide a solution for weak selection that applies to any graph or network. Our method relies on calculating the coalescence times^{10,11} of random walks¹². We evaluate large numbers of diverse population structures for their propensity to favour cooperation. We study how small changes in population structure—graph surgery—affect evolutionary outcomes. We find that cooperation flourishes most in societies that are based on strong pairwise ties.

Ecological and evolutionary dynamics depend on population structure^{13–15}. Evolutionary graph theory^{1,3,7} provides a mathematical tool for representing population structure: vertices correspond to individuals and edges indicate interactions. Graphs can describe spatially structured populations of bacteria, plants, animals¹⁶, tissue architecture in multi-cellular organisms¹⁷, or social networks^{18,19}. Graph topology affects the rate of genetic change²⁰ and the balance of drift versus selection¹. The classical setting of a well-mixed population is the complete graph.

Of particular note is the evolution of social behaviour, which can be studied using evolutionary game theory^{21–23}. Evolutionary game dynamics, which are tied to ecological dynamics²², arise whenever reproductive success is affected by interactions with others.

In evolutionary games on graphs^{3–8,24,25}, individuals interact with neighbours according to a game and reproduce on the basis of payoff (Fig. 1). A central question is to determine which strategies succeed on a given graph. In general, there cannot be a closed-form solution or polynomial-time algorithm for this question, unless it is unexpectedly found that $P = NP$ (polynomial time = nondeterministic polynomial time)⁹. To make progress, one can consider weak selection, meaning that the game has only a small effect on reproductive success. Weak selection results are known for regular graphs, where each individual has the same number of neighbours^{3–8}. Evolutionary games on heterogeneous (non-regular) graphs have only been investigated using computer simulations^{3,24,25}, approximations^{3,26} and special cases^{25,27,28}.

We consider games on any weighted graph (Fig. 1a), with edge weights w_{ij} . Individuals are of two types, A and B. The game is specified by a payoff matrix (see Methods). Each individual i plays the game with each neighbour, receiving an edge-weighted average payoff of f_i (Fig. 1b). The reproductive rate of i is $F_i = 1 + \delta f_i$, where $\delta > 0$ is the strength of selection. Weak selection means $\delta \ll 1$; neutral drift, $\delta = 0$, is a baseline.

At each time step, an individual is chosen uniformly at random to be replaced. Its neighbours compete for the vacancy proportionally to their reproductive rates (Fig. 1c). Offspring inherit the type of their parent. This update rule, called death–birth³, also translates into social settings: a random individual resolves to update its strategy, and adopts one of its neighbours' strategies proportionally to their payoff.

Over time, the population will reach the state of all A or all B. Suppose we introduce a single A at a vertex chosen uniformly at random in a population of B individuals. The fixation probability, ρ_A , is the probability of reaching all A from this initial condition. Likewise, ρ_B is the probability of reaching all B when starting with a single B individual in a population otherwise of A. Selection favours A over B if $\rho_A > \rho_B$.

The outcome of selection depends on the spatial assortment of types, which can be studied using coalescent theory^{10,11}. Ancestral lineages are represented as random walks¹². A step from i to j occurs with probability $p_{ij} = w_{ij}/w_i$, where $w_i = \sum_k w_{ik}$ is the weighted degree of vertex i . The coalescence time τ_{ij} is the expected meeting time of independent random walks started at vertices i and j (Fig. 1d), which can be obtained by solving a system of linear equations (see Methods). We show in the Supplementary Information that, if T is the time to absorption

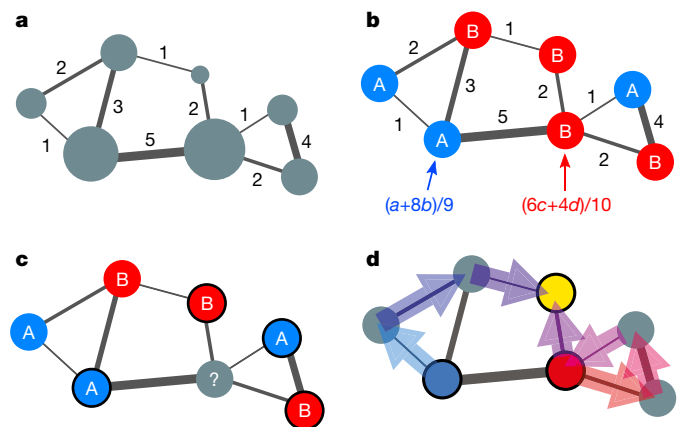


Figure 1 | Evolutionary games on weighted heterogeneous graphs. **a**, Population structure is represented by a graph with edge weights w_{ij} , which are shown next to the edges for this example. **b**, Each individual i plays a game (equation (3) in the Methods) with each neighbour, and retains the edge-weighted average payoff f_i . The reproductive rate of i is $F_i = 1 + \delta f_i$, where δ represents the strength of selection. **c**, For death–birth updating, a random individual i is selected to be replaced (indicated by a '?'); then a neighbour j is chosen with a probability proportional to $w_{ij}F_j$ to reproduce into the vacancy. **d**, The coalescence time^{10–13} τ_{ij} is the expected meeting time of random walks from i and j , representing time to a common ancestor (yellow circle).

¹Department of Mathematics, Emmanuel College, Boston, Massachusetts, USA. ²Program for Evolutionary Dynamics, Harvard University, Cambridge, Massachusetts, USA. ³Center for Mathematical Sciences and Applications, Harvard University, Cambridge, Massachusetts, USA. ⁴Department of Mathematics, Northeastern University, Boston, Massachusetts, USA. ⁵Department of Mathematics, University of Tennessee, Knoxville, Tennessee, USA. ⁶Institute for Quantitative Social Sciences, Harvard University, Cambridge, Massachusetts, USA. ⁷Department of Electrical and Computer Engineering, McGill University, Montreal, Canada. ⁸Department of Mathematics, Harvard University, Cambridge, Massachusetts, USA. ⁹Department of Organismic and Evolutionary Biology, Harvard University, Cambridge, Massachusetts, USA.

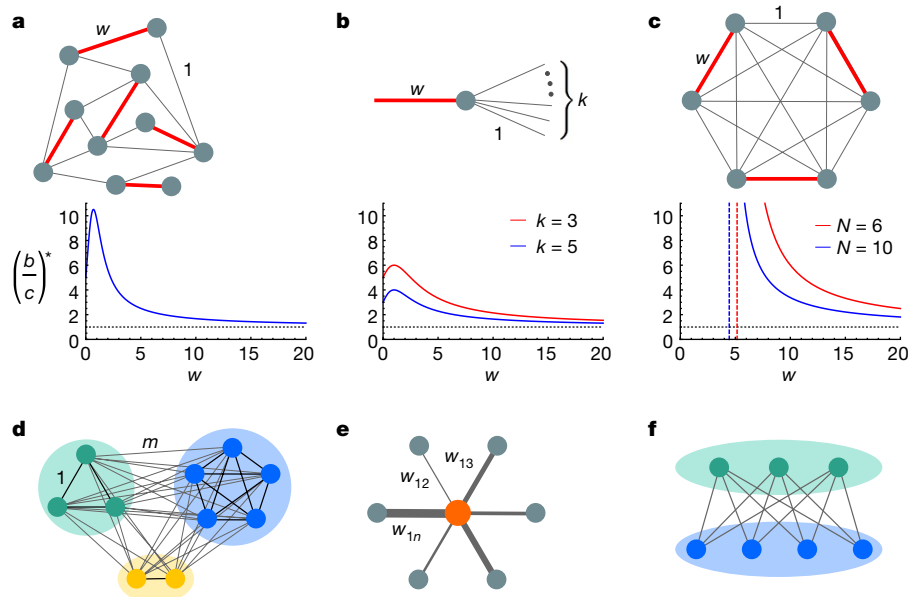


Figure 2 | Graphs that promote or hinder cooperation. **a–c**, If each individual has one partner with weight w and all other edges of weight 1, any cooperative behaviour is favoured for sufficiently large w . Examples include a disordered network (**a**); a weighted regular graph (**b**), for which $(b/c)^* = (w+k)/(w^2+k)$ for $N \gg k$; and a weighted complete graph (**c**),

for which $(b/c)^* = (w-2+N)^2/((w-2)^2-N)$; here cooperation is possible only when $w > \sqrt{N} + 2$ (dashed vertical lines). **d**, An island-structured population, with edge weights 1 within islands and $m < 1$ between islands. **e, f**, The weighted star (**e**) and the unweighted complete bipartite graph (**f**) do not support cooperation, because $t_3 = t_1$.

(fixation or extinction), then $T - \tau_{ij}$ is the expected time during which i and j have the same type. Of particular note is the expected coalescence time, t_m , from the two ends of an n -step random walk, with the initial vertex chosen proportionally to weighted degree.

Our main result holds for any payoff matrix, but we first study a donation game. Cooperators pay a cost, c , and provide a benefit, b . Defectors (that is, those who do not cooperate) pay no cost and provide no benefit. For $b > c > 0$, this game is a Prisoners' Dilemma. We find that cooperation is favoured over defection for weak selection if and only if:

$$-c(T - t_0) + b(T - t_1) > -c(T - t_2) + b(T - t_3) \quad (1)$$

Intuitively, the above condition states that a cooperator must have a higher payoff than a random individual two steps away. These two-step neighbours compete with the cooperator for opportunities to reproduce^{3,5} (Fig. 1b). The first term, $-c(T - t_0)$, is the cost for being a cooperator, which is paid for the entire time, T , because $t_0 = 0$. The second term, $b(T - t_1)$, is the average benefit that the cooperator gets from its one-step neighbours, because for expected time $T - t_1$, a one-step neighbour is also a cooperator. The remaining terms, $-c(T - t_2) + b(T - t_3)$, describe the average payoff of an individual two steps away. That individual pays cost c whenever it is a cooperator (time $T - t_2$) and receives benefit b whenever its one-step neighbours, which are three-step neighbours of the first cooperator, are cooperators (time $T - t_3$).

T cancels itself out in equation (1), leaving $-ct_2 + b(t_3 - t_1) > 0$. Therefore, cooperation is favoured under weak selection, if $t_3 > t_1$ and the benefit-to-cost ratio exceeds the threshold

$$\left(\frac{b}{c}\right)^* = \frac{t_2}{t_3 - t_1} \quad (2)$$

The critical threshold $(b/c)^*$ is obtained for any graph by solving for coalescence times and substituting into equation (2). Although equation (2) is derived in the weak selection limit, Monte Carlo simulations suggest it is accurate for fitness costs up to 2.5% (Extended Data

Fig. 1a). Therefore, the result can be used for situations of non-vanishing selection intensity, but one must ensure that selective differences are sufficiently small.

Positive $(b/c)^*$ means that cooperation is favoured when it is sufficiently effective. Positive values of $(b/c)^*$ always exceed—but can be arbitrarily close to—one, at which point any cooperation that yields a net benefit is favoured (Fig. 2a–c). Negative values arise for $t_3 < t_1$; in this case cooperation is not favoured, but spiteful behaviours, $b < 0$, $c > 0$, are favoured for $b/c < (b/c)^*$. If $t_3 = t_1$, then $(b/c)^*$ is infinite, and neither cooperation nor spite are favoured.

Which networks best facilitate evolution of cooperation? We find that cooperation thrives on networks with strong pairwise ties (Fig. 2a–c). To quantify this property, let $p_i = \sum_j p_{ij} p_{ji}$ denote the probability that a random walk from vertex i returns to i on its second step. In other words, p_i is the probability that, if i chooses a neighbour for interaction, that choice is reciprocated. Cooperation succeeds if the p_i are large. For large graphs that satisfy a locality property (see Methods), $(b/c)^* = 1/\bar{p}$, where \bar{p} is a weighted average of the p_i . If each individual has k neighbours of equal weight, then $p_i = 1/k$ for each i , yielding the condition³ $b/c > k$.

As an application, consider a population divided into islands of arbitrary sizes (Fig. 2d). Edges within an island have weight 1. Edges between islands have weight $m < 1$. We derive a closed-form expression for $(b/c)^*$ for the case of two islands. Cooperation appears to be most favoured for evenly-sized islands and a small m (see Methods and Supplementary Information).

Some population structures are not conducive to cooperation. For example, on a weighted star (Fig. 2e), one-step and three-step neighbours are equivalent; therefore $t_3 = t_1$ and cooperation is impossible. A similar argument applies to the complete bipartite graph (Fig. 2f).

In some cases, small changes in graph topology can markedly alter the fate of cooperation (Fig. 3). Stars do not support cooperation, but joining two stars via their hubs allows cooperation for $b/c > 5/2$. If we modify a star by linking pairs of leaves to obtain a 'ceiling fan', cooperation is favoured for $b/c > 8$. Therefore, targeted interventions in network structure (graph surgery) can facilitate transitions to more

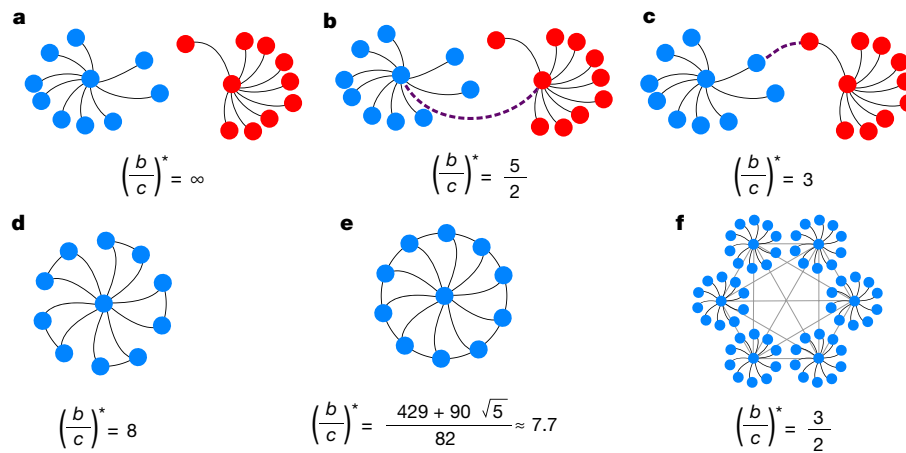


Figure 3 | Rescuing cooperation by graph surgery. **a**, The star does not support cooperation; the critical benefit–cost threshold is infinite. **b**, Joining two stars via their hubs gives $(b/c)^* = 5/2$. **c**, Joining them via two leaves gives $(b/c)^* = 3$. **d**, A ceiling fan has $(b/c)^* = 8$. **e**, A wheel has

$(b/c)^* = (429 + 90\sqrt{5})/82$. **f**, Joining m stars via their hubs in a complete graph gives $(b/c)^* = (3m - 1)/(2m - 2)$, which is approximately $3/2$ for large m . The $(b/c)^*$ values reported here are for infinite population size; see Supplementary Information for finite size.

cooperative societies. It is also of interest that a ‘dense cluster’ of stars connected by their hubs (Fig. 3f) has a benefit–cost threshold of $3/2$, which is less than its average degree of 2.

To explore the evolutionary consequences of graph topology on a large scale, we calculated $(b/c)^*$ for various ensembles: (i) 1.3 million graphs of sizes 100–150, generated by ten random graph models (Fig. 4); (ii) 40,000 graphs of sizes 300–1,000 generated by four random graph models (Extended Data Fig. 1b); (iii) every simple graph of size up to seven (Extended Data Figs 2–4); and (iv) seven empirical human and animal social networks (Extended Data Fig. 5). In general, as the average degree, \bar{k} , increases, cooperation becomes increasingly difficult and eventually impossible. However, there is considerable variance in $(b/c)^*$ for each value of \bar{k} . The propensity of a graph to support cooperation is neither determined by its average degree, nor by its entire degree sequence (Extended Data Fig. 4).

So far we have discussed the donation game, but our theory extends to any pairwise interaction; see equation (3) in the Methods. The condition for strategy A to be favoured over B, under weak selection, can be written²⁷ as $\sigma a + b > c + \sigma d$. Our result implies that $\sigma = (-t_1 + t_2 + t_3)/(t_1 + t_2 - t_3)$, from which one can evaluate the success of any strategy on any graph, under weak selection. The structure coefficient σ quantifies the extent to which a graph supports cooperation in a social dilemma, or the Pareto-efficient equilibrium in a coordination game^{2,27} (Extended Data Fig. 1c, d).

Our model can be extended in various ways. Birth–death updating³ can be studied. Total instead of average payoff can be used²⁵. Different graphs can specify interaction and replacement^{4,7,29}. Mutations can be introduced^{7,30}. For each of these variations, we obtain the conditions for success in terms of coalescence times (see Methods).

In summary, we have obtained a condition for how natural selection chooses between two competing strategies on any graph for weak selection. Our framework applies to strategic interactions among humans, as well as ecological interactions among other organisms, in any population of fixed structure (Extended Data Fig. 5). Our result helps to elucidate which population structures promote certain behaviours, such as cooperation. We find that cooperation flourishes most in the presence of strong pairwise ties, which is an intriguing argument for the importance of stable partnerships in forming the backbone of cooperative societies.

Online Content Methods, along with any additional Extended Data display items and Source Data, are available in the online version of the paper; references unique to these sections appear only in the online paper.

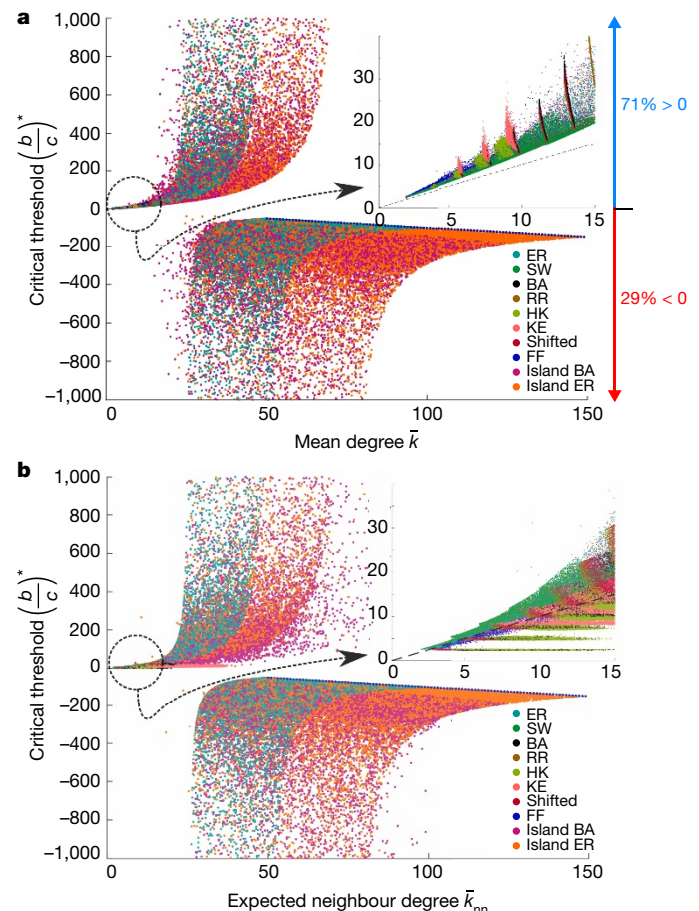


Figure 4 | Conditions for cooperation on 1.3 million random graphs. **a**, Scatter plot of critical threshold $(b/c)^*$ versus mean degree \bar{k} . 71% of graphs have positive $(b/c)^*$ and have the possibility of cooperation; negative $(b/c)^*$ indicates that spite ($b < 0, c > 0$) can be favoured. **b**, Scatter plot of $(b/c)^*$ versus \bar{k}_{nn} , the expected degree of a random neighbour of a randomly chosen vertex, which is a proposed approximation for $(b/c)^*$ on heterogeneous graphs²⁶. Although this approximation is reasonable for many graphs, there is substantial variation in $(b/c)^*$ for each value of \bar{k}_{nn} . The success of cooperation depends on features of graph topology beyond the summary statistics \bar{k} and \bar{k}_{nn} . See Methods for graph models and parameters.

Received 31 August 2016; accepted 23 February 2017.

Published online 29 March 2017.

- Lieberman, E., Hauert, C. & Nowak, M. A. Evolutionary dynamics on graphs. *Nature* **433**, 312–316 (2005).
- Nowak, M. A., Tarnita, C. E. & Antal, T. Evolutionary dynamics in structured populations. *Phil. Trans. R. Soc. B* **365**, 19–30 (2010).
- Ohtsuki, H., Hauert, C., Lieberman, E. & Nowak, M. A. A simple rule for the evolution of cooperation on graphs and social networks. *Nature* **441**, 502–505 (2006).
- Taylor, P. D., Day, T. & Wild, G. Evolution of cooperation in a finite homogeneous graph. *Nature* **447**, 469–472 (2007).
- Grafen, A. & Archetti, M. Natural selection of altruism in inelastic viscous homogeneous populations. *J. Theor. Biol.* **252**, 694–710 (2008).
- Chen, Y.-T. Sharp benefit-to-cost rules for the evolution of cooperation on regular graphs. *Ann. Appl. Probab.* **23**, 637–664 (2013).
- Allen, B. & Nowak, M. A. Games on graphs. *EMS Surv. Math. Sci.* **1**, 113–151 (2014).
- Débarre, F., Hauert, C. & Doebeli, M. Social evolution in structured populations. *Nat. Commun.* **5**, 3409 (2014).
- Ibsen-Jensen, R., Chatterjee, K. & Nowak, M. A. Computational complexity of ecological and evolutionary spatial dynamics. *Proc. Natl Acad. Sci. USA* **112**, 15636–15641 (2015).
- Kingman, J. F. C. The coalescent. *Stochastic Process. Appl.* **13**, 235–248 (1982).
- Wakeley, J. *Coalescent Theory: an Introduction*. (Roberts and Company Publishers, 2009).
- Cox, J. T. Coalescing random walks and voter model consensus times on the torus in \mathbb{Z}^d . *Ann. Probab.* **17**, 1333–1366 (1989).
- Durrett, R. & Levin, S. The importance of being discrete (and spatial). *Theor. Popul. Biol.* **46**, 363–394 (1994).
- Hassell, M. P., Comins, H. N. & May, R. M. Species coexistence and self-organizing spatial dynamics. *Nature* **370**, 290–292 (1994).
- Nowak, M. A. & May, R. M. Evolutionary games and spatial chaos. *Nature* **359**, 826–829 (1992).
- Allen, B., Gore, J. & Nowak, M. A. Spatial dilemmas of diffusible public goods. *eLife* **2**, e011169 (2013).
- Nowak, M. A., Michor, F. & Iwasa, Y. The linear process of somatic evolution. *Proc. Natl Acad. Sci. USA* **100**, 14966–14969 (2003).
- Santos, F. C., Santos, M. D. & Pacheco, J. M. Social diversity promotes the emergence of cooperation in public goods games. *Nature* **454**, 213–216 (2008).
- Rand, D. G., Nowak, M. A., Fowler, J. H. & Christakis, N. A. Static network structure can stabilize human cooperation. *Proc. Natl Acad. Sci. USA* **111**, 17093–17098 (2014).
- Allen, B. *et al.* The molecular clock of neutral evolution can be accelerated or slowed by asymmetric spatial structure. *PLoS Comput. Biol.* **11**, e1004108 (2015).
- Maynard Smith, J. *Evolution and the Theory of Games* (Cambridge Univ. Press, 1982).
- Hofbauer, J. & Sigmund, K. *Evolutionary Games and Replicator Dynamics* (Cambridge Univ. Press, 1998).
- Broom, M. & Rychtář, J. *Game-Theoretical Models in Biology*. (Chapman and Hall/CRC, 2013).
- Santos, F. C. & Pacheco, J. M. Scale-free networks provide a unifying framework for the emergence of cooperation. *Phys. Rev. Lett.* **95**, 098104 (2005).
- Maciejewski, W., Fu, F. & Hauert, C. Evolutionary game dynamics in populations with heterogeneous structures. *PLOS Comput. Biol.* **10**, e1003567 (2014).
- Konno, T. A condition for cooperation in a game on complex networks. *J. Theor. Biol.* **269**, 224–233 (2011).
- Tarnita, C. E., Ohtsuki, H., Antal, T., Fu, F. & Nowak, M. A. Strategy selection in structured populations. *J. Theor. Biol.* **259**, 570–581 (2009).
- Hadjichrysanthou, C., Broom, M. & Rychtář, J. Evolutionary games on star graphs under various updating rules. *Dyn. Games App.* **1**, 386–407 (2011).
- Ohtsuki, H., Nowak, M. A. & Pacheco, J. M. Breaking the symmetry between interaction and replacement in evolutionary dynamics on graphs. *Phys. Rev. Lett.* **98**, 108106 (2007).
- Allen, B., Traulsen, A., Tarnita, C. E. & Nowak, M. A. How mutation affects evolutionary games on graphs. *J. Theor. Biol.* **299**, 97–105 (2012).

Supplementary Information is available in the online version of the paper.

Acknowledgements This work was supported by Office of Naval Research grant N00014-16-1-2914, the John Templeton Foundation, a gift from B. Wu and E. Larson, AFOSR grant FA9550-13-1-0097 (G.L.), the James S. McDonnell Foundation (B.F.), and the Center for Mathematical Sciences and Applications at Harvard University (B.A., Y.-T.C.). We are grateful to S. R. Sundaresan and D. I. Rubenstein for providing data on zebra and wild ass networks, and for discussions.

Author Contributions B.A., G.L., Y.-T.C. and M.A.N. conceived the project. B.A., G.L., Y.-T.C. and S.-T.Y. performed mathematical analysis. N.M., B.F. and G.L. performed numerical experiments and Monte Carlo simulations. B.A. and M.A.N. wrote the paper. All authors contributed to all aspects of the project.

Author Information Reprints and permissions information is available at www.nature.com/reprints. The authors declare no competing financial interests. Readers are welcome to comment on the online version of the paper. Publisher's note: Springer Nature remains neutral with regard to jurisdictional claims in published maps and institutional affiliations. Correspondence and requests for materials should be addressed to B.A. (allenb@emmanuel.edu).

METHODS

Here we summarize our model and mathematical methods; see Supplementary Information for complete derivations. No experiments were performed for this study, and no empirical data were collected.

Model. Population structure is represented by a weighted, connected graph of size N . Consistent with standard mathematical terminology, a ‘graph’ is understood to be undirected. The edge weight between vertices i and j is denoted $w_{ij} = w_{ji}$. Self-loops ($w_{ii} > 0$) are allowed, representing self-interaction and replacement by one’s own offspring. The weighted degree of vertex i is $w_i = \sum_j w_{ij}$.

Individuals are one of two types, corresponding to strategies in a game. The payoff matrix of a 2×2 game can be written as

$$\begin{matrix} & \text{A} & \text{B} \\ \text{A} & \begin{pmatrix} a & b \end{pmatrix} \\ \text{B} & \begin{pmatrix} c & d \end{pmatrix} \end{matrix} \quad (3)$$

For the donation game, the payoff matrix is

$$\begin{matrix} & \text{C} & \text{D} \\ \text{C} & \begin{pmatrix} b-c & -c \end{pmatrix} \\ \text{D} & \begin{pmatrix} b & 0 \end{pmatrix} \end{matrix} \quad (4)$$

The state of the process is given by the vector (s_1, \dots, s_N) , where $s_i \in \{0,1\}$ indicates the type occupying each vertex: 1 for A and 0 for B in the game of equation (3); 1 for C and 0 for D in the donation game of equation (4). In each state, each individual i retains the edge-weighted average, f_i , of the payoff received from each neighbour. For the donation game of equation (4), we have $f_i = -cs_i + b \sum_j p_{ij} s_j$. The reproductive rate of i is $F_i = 1 + \delta f_i$, where $\delta \ll 1$ is the intensity of selection.

For death–birth updating, after the game interaction, an individual is selected, uniformly at random, to be replaced. A neighbour is then chosen, with probability proportional to reproductive rate times edge weight, to reproduce into the vacancy. Thus, if i is chosen to be replaced, the probability that j reproduces is $w_{ij} F_j / (\sum_k w_{ik} F_k)$. Offspring inherit the type of the parent, resulting in a new state.

Coalescence times. The coalescence times^{12,31} τ_{ij} are the solution to the system of linear equations

$$\tau_{ij} = \begin{cases} 1 + \frac{1}{2} \sum_k (p_{ik} \tau_{jk} + p_{jk} \tau_{ik}) & i \neq j \\ 0 & i = j \end{cases} \quad (5)$$

Equation (5) can be solved for any graph, in polynomial time, using standard methods. From the coalescence times, pairwise statistics of assortment can be obtained using the formula

$$\left\langle \frac{1}{N} - s_i s_j \right\rangle = \frac{\tau_{ij}}{2N} \quad (6)$$

Above, the brackets $\langle \rangle$ indicate an expectation over states arising under neutral drift, $\delta = 0$.

The n -step coalescence time is defined as $t_n = \sum_{i,j} \pi_i p_{ij}^{(n)} \tau_{ij}$, where $p_{ij}^{(n)}$ is the probability that an n -step random walk starting at i terminates at j and $\pi_i = w_i / \sum_j w_j$ is the relative weighted degree of vertex i .

Derivation of equation (1). Applying recent results on perturbations of voter models⁶, we express the fixation probability of cooperation in the donation game of equation (4) as

$$\rho_C = \frac{1}{N} + \delta \sum_i \pi_i (-c(s_i s_i^{(0)} - s_i s_i^{(2)}) + b(s_i s_i^{(1)} - s_i s_i^{(3)})) + \mathcal{O}(\delta^2) \quad (7)$$

Above, $s_i^{(n)}$ = $\sum_j p_{ij}^{(n)} s_j$ is the expected type at the end of an n -step random walk from i . Combining equations (6) and (7), we obtain

$$\rho_C = \frac{1}{N} + \frac{\delta}{2N} (-ct_2 + b(t_3 - t_1)) + \mathcal{O}(\delta^2) \quad (8)$$

Equations (1) and (2) of the main text follow immediately.

Derivation of $(b/c)^* = 1/\bar{p}$. From equation (5) we obtain the recurrence relation

$$t_{n+1} = t_n + \sum_i \pi_i p_{ii}^{(n)} \tau_i - 1 \quad (9)$$

Above, $\tau_i = 1 + \sum_j p_{ij} \tau_{ij}$ is the re-meeting time of two independent random walks from vertex i . For graphs with no self-loops ($p_{ii}^{(1)} = 0$ for each i), equation (9) gives $t_2 = \sum_i \pi_i \tau_i - 2$ and $t_3 - t_1 = \sum_i \pi_i p_i \tau_i - 2$, where p_i is shorthand for $p_{ii}^{(2)}$. Equation (2) then becomes

$$\left(\frac{b}{c}\right)^* = \frac{\sum_i \pi_i \tau_i - 2}{\sum_i \pi_i p_i \tau_i - 2} \quad (10)$$

For a regular graphs of degree k , we find that $p_i = 1/k$ for each vertex i and $\sum_i \pi_i \tau_i = N$, yielding the condition^{4,6,7} $b/c > (N-2)/(N/k-2)$.

We say that a large graph has the ‘locality property’ if $\pi_i/p_i \ll 1$ for each vertex i . This condition asserts that the (global) probability π_i of choosing i from among all vertices, proportionally to weighted degree, is eclipsed by the (local) probability p_i of reaching i by a random step from a random neighbour. We prove in the Supplementary Information that for graphs with this property, the 2’s in the numerator and denominator of equation (10) are negligible. This leads to $(b/c)^* = 1/\bar{p}$, where $\bar{p} = \sum_i \pi_i p_i \tau_i / (\sum_i \pi_i \tau_i)$ is the weighted average of the p_i with weights $\pi_i \tau_i$.

Islands. In the island model, edge weights are $w_{ij} = 1$ if i and j are on the same island and $w_{ij} = m < 1$ otherwise. For two islands with $m \ll 1$ we obtain

$$\left(\frac{b}{c}\right)^* = \frac{N^2(N-2)^3 + N(N^2 - 7N + 8)D^2 + (2N-3)D^4}{4N(N-2)(N-D^2)}$$

Above, N is the total population size and D is the difference in island sizes. The critical b/c ratio is minimized when $D = 0$; that is, when the islands have equal size. The result for arbitrary m is given in the Supplementary Information, and results for up to five islands are discussed there as well. These results suggest that, for any fixed number n of islands, cooperation is most favoured when the islands have equal size, in which case $(b/c)^* = (N-2)(N-n)/(Nn-2N+2n)$.

Arbitrary games. We extend to the general 2×2 matrix game of equation (3) using the Structure Coefficient Theorem²⁷. This theorem states that the condition for A to be favoured over B (in the sense that $\rho_A > \rho_B$ under weak selection) takes the form $\sigma a + b > c + \sigma d$. The structure coefficient σ can be calculated as $\sigma = ((b/c)^* + 1) / ((b/c)^* - 1)$, leading to $\sigma = (-t_1 + t_2 + t_3) / (t_1 + t_2 - t_3)$ as stated in the main text. We prove in the Supplementary Information that the numerator and denominator of σ are always positive.

Accumulated payoffs. Accumulated payoff means that the reproductive rate is based on the edge-weighted total payoff received from neighbours (instead of the edge-weighted average). For the donation game of equation (4), the accumulated payoff to vertex i is $f_i = -cs_i + b \sum_j w_{ij} s_j$. A similar derivation leads to

$$\left(\frac{b}{c}\right)^* = \frac{\sum_{i,j} \pi_i^2 p_{ij}^{(2)} \tau_{ij}}{\sum_{i,j,k} \pi_i^2 p_{ij}^{(2)} p_{ik} (\tau_{jk} - \tau_{ik})} \quad (11)$$

Different interaction and replacement graphs. We can also suppose that individuals interact according to one graph I and reproduce according to another graph G . Equation (2) then generalizes to

$$\left(\frac{b}{c}\right)^* = \frac{t_{2,0}}{t_{2,1} - t_{0,1}} \quad (12)$$

Above, $t_{n,m}$ is the expected coalescence time between two ends of a random walk, where the initial vertex is chosen with probability π_i , then n steps are taken in the replacement graph, and finally m steps are taken in the interaction graph. The relative weighted degree π_i and the coalescence times are computed according to the replacement graph.

Birth–death updating. For birth–death updating³, first an individual i is chosen to reproduce proportionally to its reproductive rate F_i . The offspring replaces a neighbour j chosen proportionally to w_{ij} . Birth–death requires a modified coalescent process, in which steps from i to j occur at rate w_{ij}/w_j . We denote the modified coalescence times by $\tilde{\tau}_{ij}$; these are again the unique solution to a system of linear equations (see Supplementary Information). The critical benefit–cost ratio for birth–death is

$$\left(\frac{b}{c}\right)^* = \frac{\sum_{i,j} \frac{w_{ij}}{w_i w_j} \tilde{\tau}_{ij}}{\sum_{i,j,k} \frac{w_{ij} w_{ik}}{w_i^2 w_j} (\tilde{\tau}_{jk} - \tilde{\tau}_{ik})} \quad (13)$$

Mutation. We introduce mutations with arbitrary probability u per reproduction. Mutations are equally likely to result in either type (including that of the parent). Spatial assortment is analysed using identity-by-descent^{4,7,30,32,33}. Two individuals are identical-by-descent (IBD) if no mutation separates either from their common

ancestor. The stationary probability that individuals i and j are IBD is denoted q_{ij} . The IBD probabilities q_{ij} satisfy the linear recurrence relations^{7,30}:

$$q_{ij} = \begin{cases} 1 & i = j \\ \frac{1-u}{2} \sum_k (p_{ik}q_{jk} + p_{jk}q_{ik}) & i \neq j \end{cases} \quad (14)$$

From equation (14), all IBD probabilities can be computed for any mutation rate u on any graph in polynomial time. Let $q_n = \sum_i \pi_i p_{ij}^{(n)} q_{ij}$ denote the expected IBD probability for the two ends of an n -step random walk, with initial vertex i chosen with probability π_i . We show in the Supplementary Information that cooperation is favoured, in the sense of having stationary frequency $>50\%$, when b/c exceeds the critical ratio of

$$\left(\frac{b}{c}\right)^* = \frac{1-q_2}{q_1-q_3} \quad (15)$$

Random graph investigations. For Fig. 4 we computed $(b/c)^*$ for 1.3 million unweighted graphs, generated from 10 different random graph models. Parameter values were sampled from a uniform distribution on the specified ranges (see below). Initial graph sizes were uniformly sampled in the range $100 \leq N \leq 150$; if the random graph model produced a disconnected graph, the largest connected component was used. The critical $(b/c)^*$ ratio was computed by solving equation (5) for coalescence times and substituting into equation (10). (No Monte Carlo simulations were used for these investigations.)

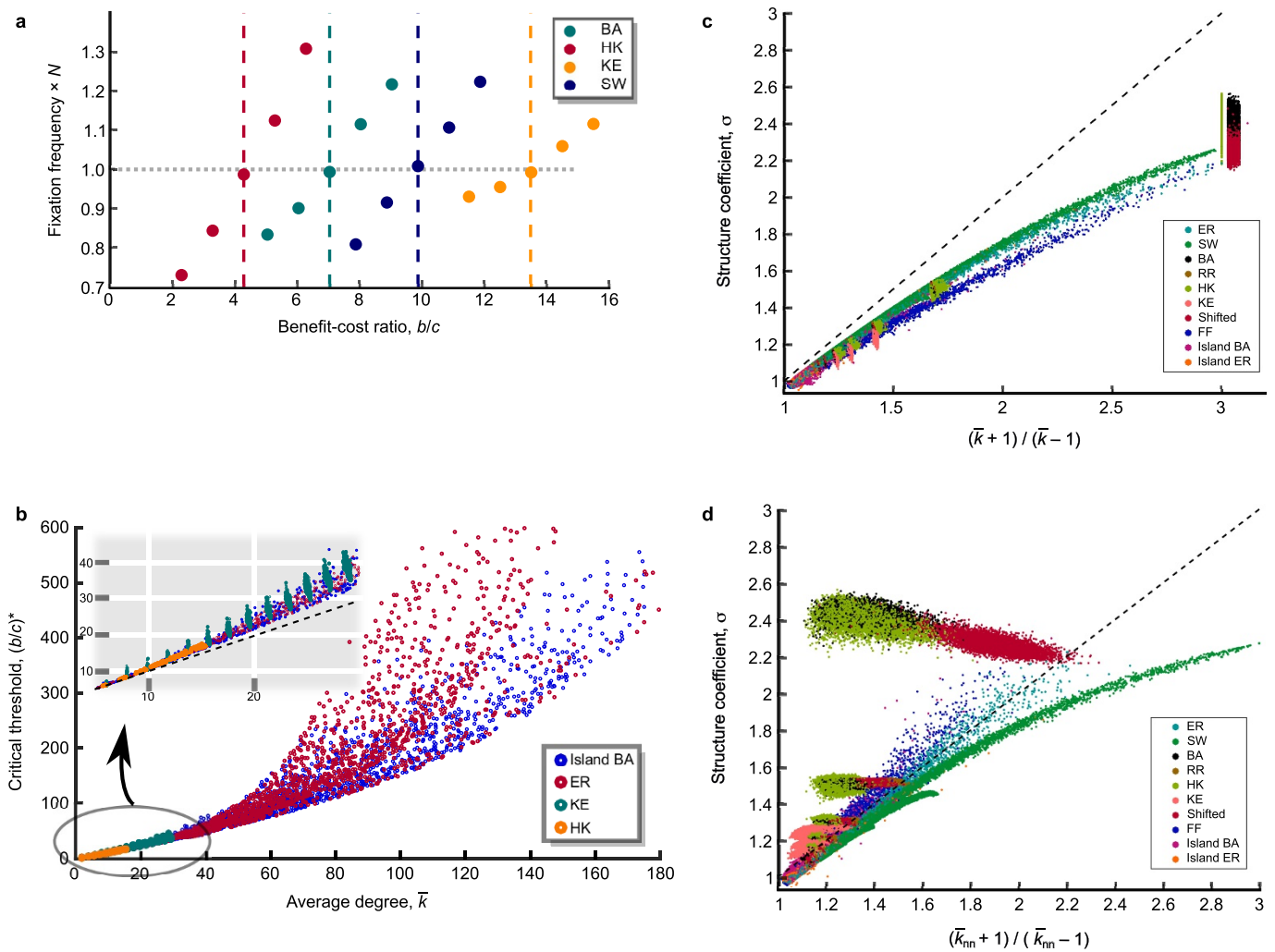
Random graph models and parameter ranges (see Fig. 4 and Extended Data Fig. 1) are as follows: 100,000 Erdős–Rényi (ER)³⁴ with edge probability $0 < p < 1$; 100,000 small world (SW)³⁵ with initial connection distance $1 \leq d \leq 5$ and edge creation probability $0 < p < 0.05$; 100,000 Barabási–Albert (BA)³⁶ with linking number $1 \leq m \leq 10$; 100,000 random recursive (RR)³⁷ (like Barabási–Albert except that edges are added uniformly instead of preferentially) with linking number $2 \leq m \leq 8$; 200,000 Holme–Kim (HK)³⁸ with linking number $2 \leq m \leq 4$ and triad formation parameter $0 < p < 0.15$; 200,000 Klemm–Eguiluz (KE)³⁹ with linking number $3 \leq m \leq 5$ and deactivation parameter $0 < \mu < 0.15$; 200,000 shifted-linear preferential attachment⁴⁰ with linking number $1 \leq m \leq 7$ and shift $0 < \theta < 40$; 100,000 forest fire (FF)⁴¹ with parameters $0 < p_f < p_b < 0.15$; 100,000 Island Barabási–Albert; and 100,000 Island Erdős–Rényi. Island Barabási–Albert is a meta-network of islands⁴², in which each island is a shifted-linear preferential attachment network with the same parameters as above. The number of islands varies from 2 to 5. Considering the islands as meta-nodes, the meta-network among the islands is an Erdős–Rényi graph with edge probability $0 < p_{\text{inter}} < 1$. Island Erdős–Rényi is the same as Island Barabási–Albert, except that each island is an Erdős–Rényi graph with edge probability $0 < p_{\text{intra}} < 1$.

Code availability. Code that supports the findings of this study is available in Zenodo with the identifier <http://dx.doi.org/10.5281/zenodo.276933>.

Data availability. This study analysed publicly available datasets from the Stanford Large Network Dataset Collection, <http://snap.stanford.edu/data/>, and the Koblenz

Network Collection, <http://konect.uni-koblenz.de/>, as well as datasets provided by S. R. Sundaresan and D. I. Rubenstein, which are available upon request from D. I. Rubenstein (dir@princeton.edu).

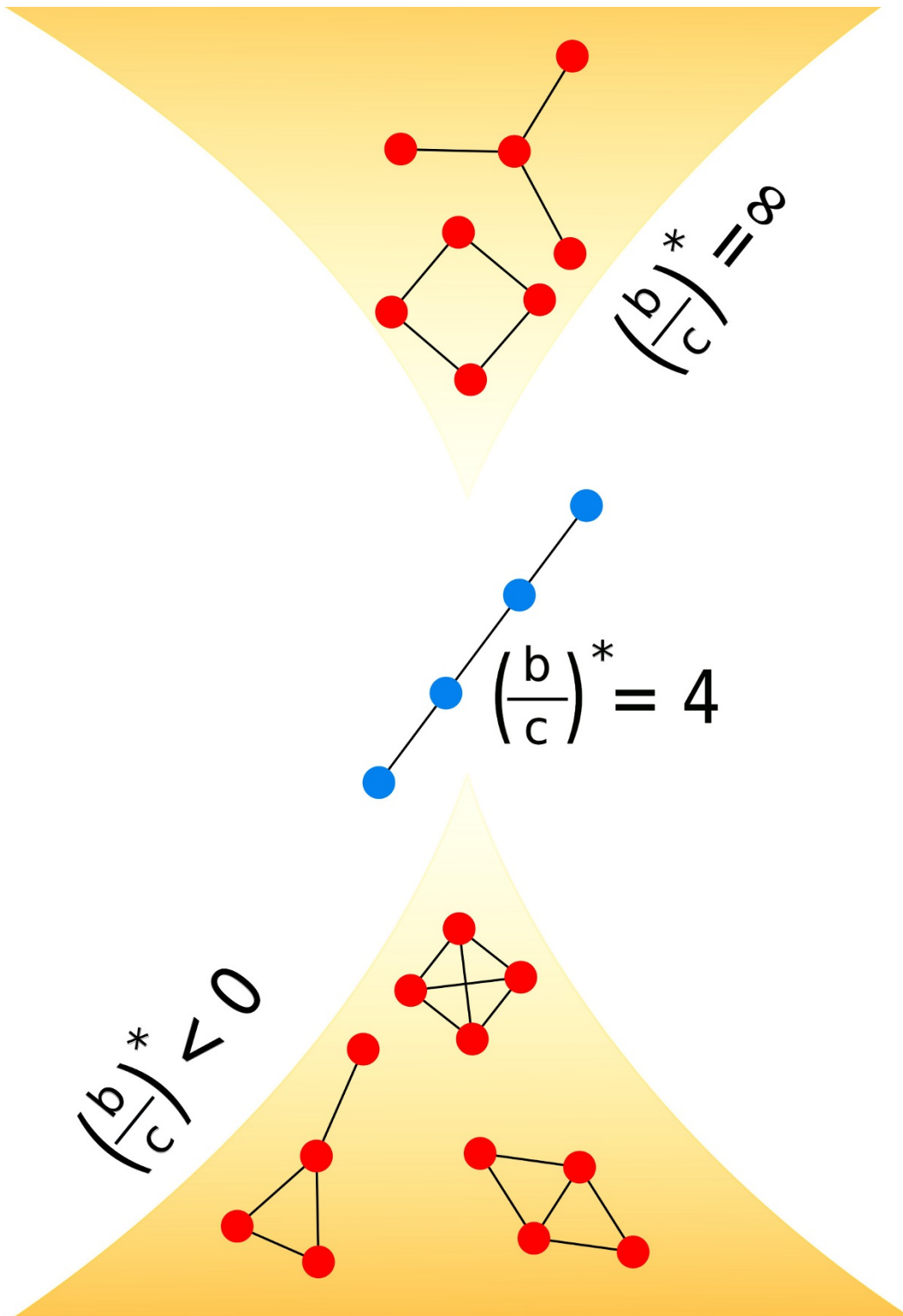
31. Liggett, T. M. *Interacting Particle Systems* (Springer Science and Business Media, 2006).
32. Malécot, G. *Les Mathématiques de l'Hérédité*. (Masson et Cie, 1948).
33. Slatkin, M. Inbreeding coefficients and coalescence times. *Genet. Res.* **58**, 167–175 (1991).
34. Erdős, P. & Rényi, A. On random graphs I. *Publ. Math. (Debrecen)* **6**, 290–297 (1959).
35. Newman, M. E. J. & Watts, D. J. Renormalization group analysis of the small-world network model. *Phys. Lett. A* **263**, 341–346 (1999).
36. Barabási, A.-L. & Albert, R. Emergence of scaling in random networks. *Science* **286**, 509–512 (1999).
37. Dorogovtsev, S. N., Goltsev, A. V. & Mendes, J. F. F. Critical phenomena in complex networks. *Rev. Mod. Phys.* **80**, 1275 (2008).
38. Holme, P. & Kim, B. J. Growing scale-free networks with tunable clustering. *Phys. Rev. E* **65**, 026107 (2002).
39. Klemm, K. & Eguiluz, V. M. Highly clustered scale-free networks. *Phys. Rev. E* **65**, 036123 (2002).
40. Krapivsky, P. L. & Redner, S. Organization of growing random networks. *Phys. Rev. E* **63**, 066123 (2001).
41. Leskovec, J., Kleinberg, J. & Faloutsos, C. Graphs over time: densification laws, shrinking diameters and possible explanations. In *Proc. 11th ACM SIGKDD International Conference on Knowledge Discovery in Data Mining* 177–187 (ACM, 2005).
42. Lozano, S., Arenas, A. & Sánchez, A. Mesoscopic structure conditions the emergence of cooperation on social networks. *PLoS One* **3**, e1892 (2008).
43. Gore, J., Youk, H. & van Oudenaarden, A. Snowdrift game dynamics and facultative cheating in yeast. *Nature* **459**, 253–256 (2009).
44. Lusseau, D. et al. The bottlenose dolphin community of Doubtful Sound features a large proportion of long-lasting associations. *Behav. Ecol. Sociobiol.* **54**, 396–405 (2003).
45. Sade, D. S. Sociometrics of *Macaca mulatta*. I. Linkages and cliques in grooming matrices. *Folia Primatol. (Basel)* **18**, 196–223 (1972).
46. Sundaresan, S. R., Fischhoff, I. R., Dushoff, J. & Rubenstein, D. I. Network metrics reveal differences in social organization between two fission–fusion species, Grevy's zebra and onager. *Oecologia* **151**, 140–149 (2007).
47. Hill, A. L., Rand, D. G., Nowak, M. A. & Christakis, N. A. Infectious disease modeling of social contagion in networks. *PLoS Comput. Biol.* **6**, e1000968 (2010).
48. Christakis, N. A. & Fowler, J. H. The spread of obesity in a large social network over 32 years. *N. Engl. J. Med.* **357**, 370–379 (2007).
49. McAuley, J. J. & Leskovec, J. Learning to discover social circles in ego networks. *Adv. Neural Inf. Process. Syst.* **25**, 548–556 (2012).
50. Leskovec, J., Kleinberg, J. & Faloutsos, C. Graph evolution: densification and shrinking diameters. *ACM Trans. Knowl. Discov. Data* **1**, 2 (2007).
51. Hauert, C., Michor, F., Nowak, M. A. & Doebeli, M. Synergy and discounting of cooperation in social dilemmas. *J. Theor. Biol.* **239**, 195–202 (2006).
52. Nowak, M. A. Evolving cooperation. *J. Theor. Biol.* **299**, 1–8 (2012).



Extended Data Figure 1 | Further numerical and simulation results.

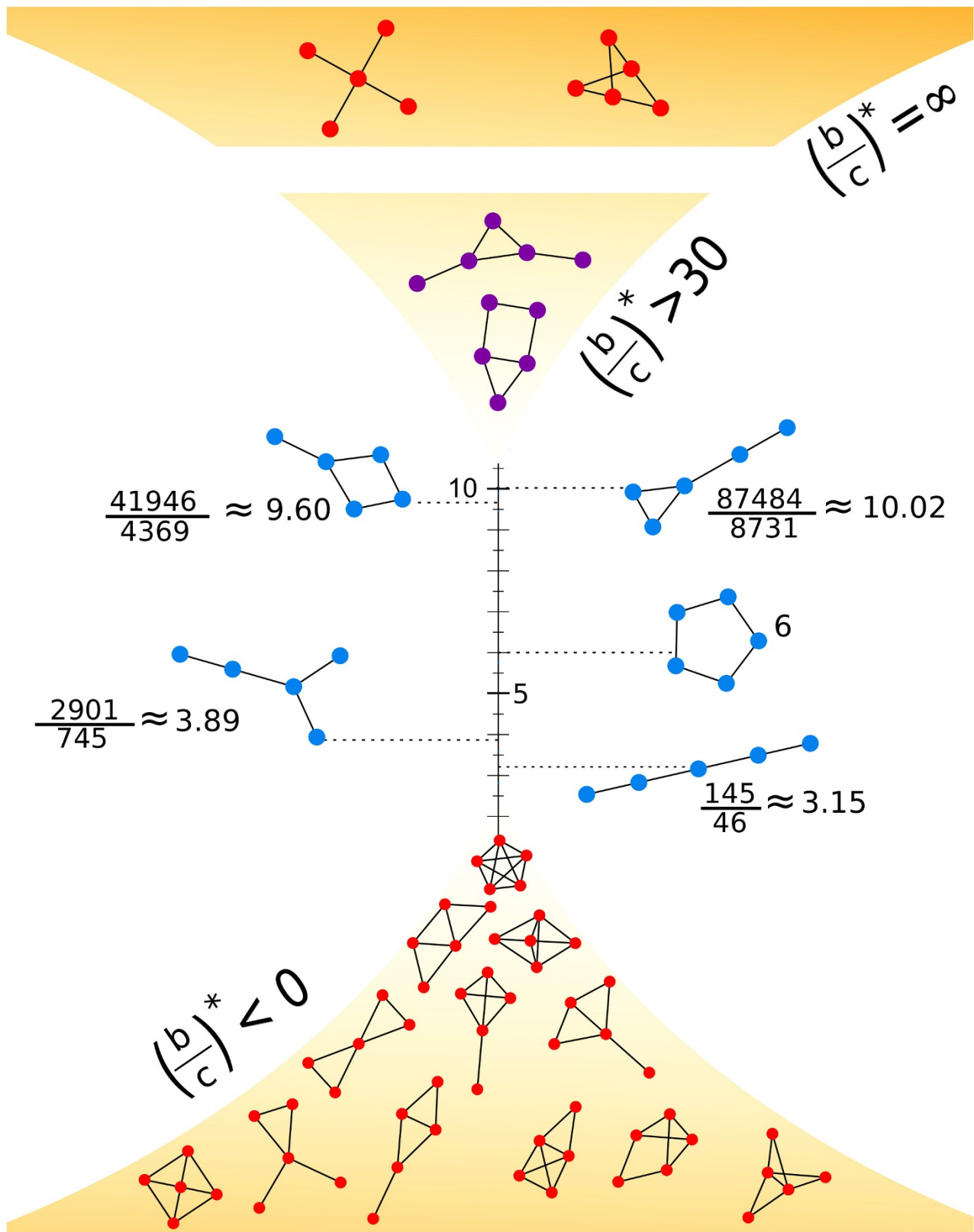
a, To assess accuracy of our results for empirically plausible selection strength, we performed Monte Carlo simulations with $\delta = 0.025$ and $c = 1$. This corresponds to a fitness cost of 2.5%, which was determined to be the cost of cooperative behaviour in yeast⁴³. Markers indicate population size times frequency of fixation for a particular value of b on a particular graph. Dashed lines indicate $(b/c)^*$ as calculated from equation (2). All graphs have size $N = 100$. Graphs are: Barabási-Albert (BA) with linking number $m = 3$, small world³⁵ (SW) with initial connection distance $d = 3$ and edge creation probability $p = 0.025$, Klemm-Eguiluz³⁹ (KE) with linking number $m = 5$ and deactivation parameter $\mu = 0.2$, and Holme-Kim³⁸ (HK) with linking number $m = 2$ and triad formation parameter $P = 0.2$. **b**, We computed $(b/c)^*$ for 4×10^4 large random graphs (sizes 300–1,000) using four random graph models: Erdős-Rényi³⁴ (ER) with edge

probability $0 < p < 0.25$, Klemm-Eguiluz with linking number $3 \leq m \leq 5$ and deactivation parameter $0 < \mu < 0.15$, Holme-Kim with linking number $2 \leq m \leq 4$ and triad formation parameter $0 < P < 0.15$, and a meta-network⁴² of shifted-linear preferential attachment networks⁴⁰ (Island Barabási-Albert) with $0 < p_{\text{inter}} < 0.25$; see Methods for details. **c**, **d**, We computed the structure coefficient²⁷ $\sigma = ((b/c)^* + 1) / ((b/c)^* - 1)$ for the same ensemble of random graphs as in Fig. 4 of the main text. Strategy A is favoured over strategy B under weak selection if $\sigma a + b > c + \sigma d$; see equation (3) of Methods. **c**, Plot of σ versus $(\bar{k} + 1) / (\bar{k} - 1)$, which is the σ -value for a regular graph of the same mean degree \bar{k} . **d**, Plot of σ versus $(\bar{k}_{nn} + 1) / (\bar{k}_{nn} - 1)$, which is the σ -value one would expect if the condition $b/c > \bar{k}_{nn}$ (as described in ref. 26) were exact. Here, \bar{k}_{nn} is the expected degree of a neighbour of a randomly chosen vertex.

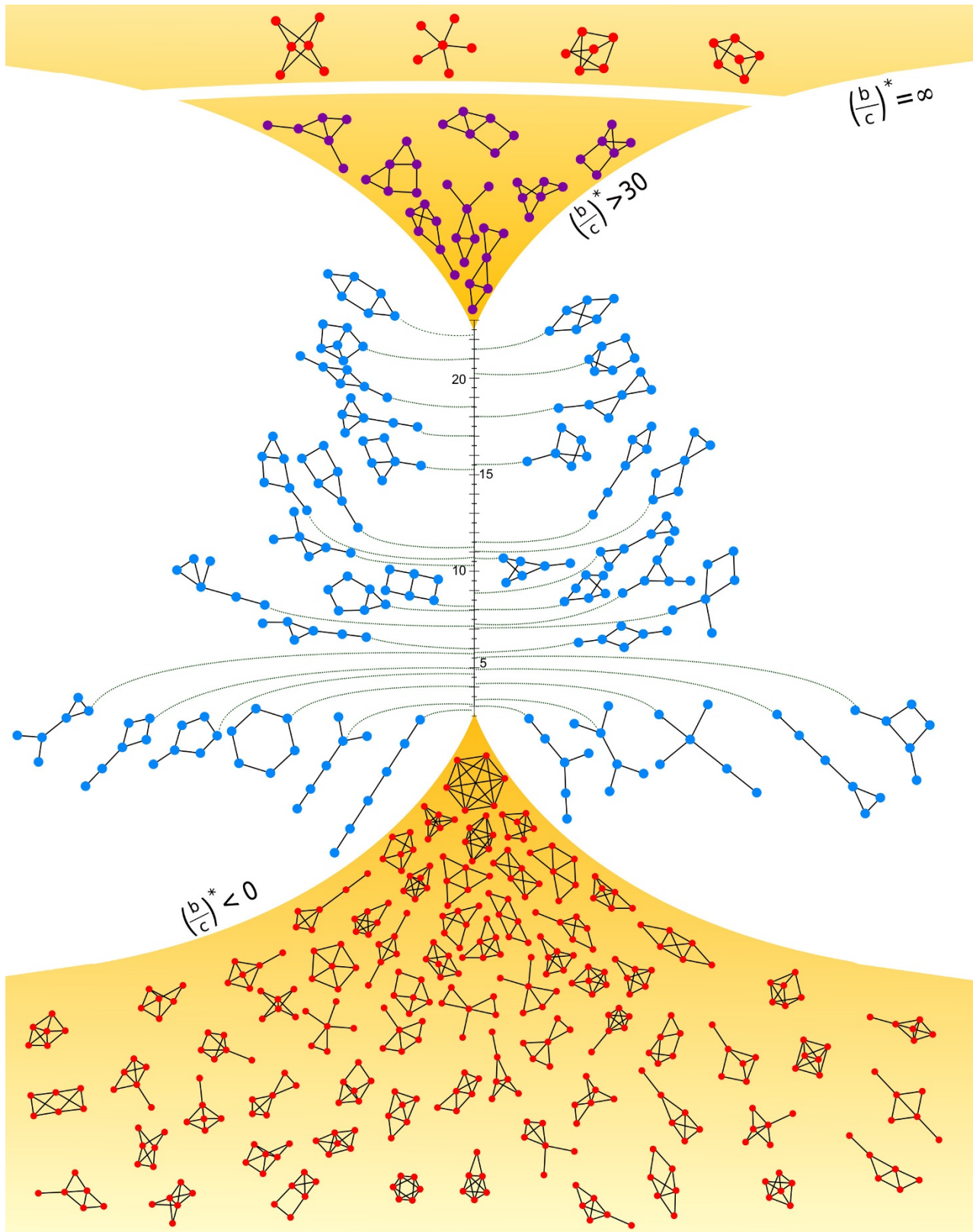


Extended Data Figure 2 | The critical benefit–cost threshold for all graphs of size four. There are six connected, unweighted graphs of size four. Of these, only the path graph has positive $(b/c)^*$. Two others have

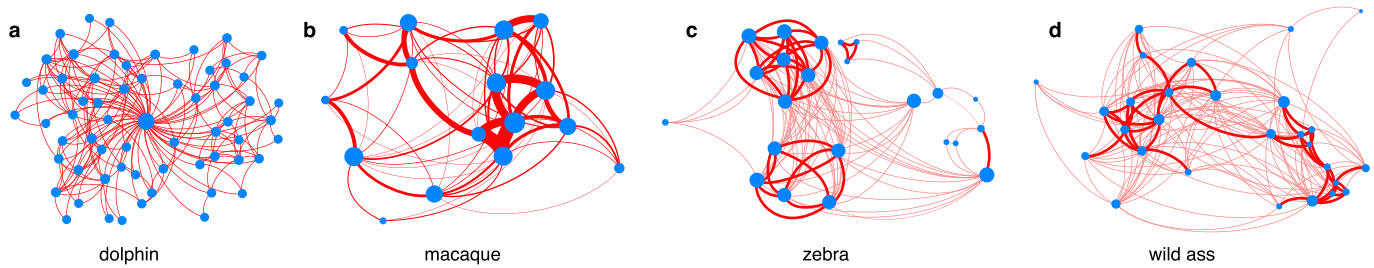
infinite $(b/c)^*$ and three have negative $(b/c)^*$. For size three (not shown), there are only two connected, unweighted graphs: the path, which has $(b/c)^* = \infty$, and the triangle, which has $(b/c)^* = -2$.



Extended Data Figure 3 | The critical benefit–cost threshold for all graphs of size five. There are 21 connected, unweighted graphs of size five. Critical ratios in the range $0 < (b/c)^* < 30$ are shown. Overall, seven of the $(b/c)^*$ values are positive, twelve are negative, and two are infinite.



Extended Data Figure 4 | The critical benefit–cost threshold for all graphs of size six. There are 112 connected, unweighted graphs of size six. Of these, 43 have positive $(b/c)^*$, 65 have negative $(b/c)^*$, and four have $(b/c)^* = \infty$. Notably, there are graphs with the same degree sequence (for example, 3, 2, 2, 1, 1, 1) but different $(b/c)^*$.



e

Population	Network	Weighted?	N	\bar{k}	$(b/c)^*$	σ
Bottlenose dolphin	frequent association	no	62	5.1	6.5	1.36
Rhesus macaque	grooming	yes	16	–	21.0	1.1
Grevy's zebra	group association	yes	23	–	6.1	1.39
Asiatic wild ass	group association	yes	28	–	5.6	1.43
Framingham study	family, coworkers, friends	no	5253	6.5	7.7	1.30
Facebook users	online friends	no	4039	43.7	48.5	1.04
arXiv:gr-qc authors	co-authorship	no	4159	6.5	6.6	1.36

Extended Data Figure 5 | Results for empirical networks. The benefit–cost threshold $(b/c)^*$, or equivalently the structure coefficient^{2,27} σ , gives the propensity of a population structure to support cooperative and/or Pareto-efficient behaviours. These values should be interpreted in terms of specific behaviours occurring in a population, and they depend on the network ontology (that is, the meaning of links). They can be used to facilitate comparisons across populations of similar species, or to predict consequences of changes in population structure. **a**, Unweighted social network of frequent associations in bottlenose dolphins (*Tursiops* spp.)⁴⁴. **b**, Grooming interaction network in rhesus macaques (*Macaca mulatta*), weighted by grooming frequency⁴⁵. **c**, Weighted network of group association in Grevy's zebras (*Equus grevyi*)⁴⁶. Preferred associations, which are statistically more frequent than random, are given weight 1. Other associations occurring at least once are given weight $\epsilon \ll 1$. **d**, Weighted network of group association in Asiatic wild asses (onagers)⁴⁶, with the same weighting scheme as for the zebra network. For both zebra

and wild ass, the unweighted networks, including every association ever observed, are dense and behave like well-mixed populations. By contrast, the weighted networks, which emphasize close ties, can promote cooperation. **e**, Table showing data from **a–d** as well as a social network of family, self-reported friends, and co-workers as of 1971 from the Framingham Heart Study^{47,48}, a Facebook ego-network⁴⁹, and the co-authorship network for the General Relativity (gr) and Quantum Cosmology (qc) category of the arXiv preprint server⁵⁰. Average degree is reported for unweighted graphs only; for weighted graphs it is unclear which notion of degree is most relevant. Note that large $(b/c)^*$ ratios, which correspond to σ values close to one, do not mean that cooperation is never favoured. Rather, the implication is that the network behaves similarly to a large well-mixed population, for which cooperation is favoured for any 2×2 game with $a + b > c + d$. The donation game does not satisfy this inequality, but other cooperative interactions do^{51,52}.